

Breathing Pyrochlore Lattice Realized in *A*-Site Ordered Spinel Oxides $\text{LiGaCr}_4\text{O}_8$ and $\text{LiInCr}_4\text{O}_8$

Yoshihiko Okamoto^{1,*}, Gøran J. Nilsen^{1,†}, J. Paul Attfield², and Zenji Hiroi¹

¹*Institute for Solid State Physics,*

University of Tokyo, Kashiwa 277-8581, Japan

²*Centre for Science at Extreme Conditions and School of Chemistry,*

University of Edinburgh,

Edinburgh EH9 3JZ, United Kingdom

(Dated: August 31, 2018)

A unique type of frustrated lattice is found in two *A*-site ordered spinel oxides, $\text{LiGaCr}_4\text{O}_8$ and $\text{LiInCr}_4\text{O}_8$. Because of the large size mismatch between Li^+ and $\text{Ga}^{3+}/\text{In}^{3+}$ ions at the *A* site, the pyrochlore lattice, made up of Cr^{3+} ions carrying spin $3/2$, becomes an alternating array of small and large tetrahedra, i.e., a “breathing” pyrochlore lattice. We introduce a parameter, the breathing factor B_f , which quantifies the degree of frustration in the pyrochlore lattice: B_f is defined as J'/J , where J' and J are nearest-neighbor magnetic interactions in the large and small tetrahedra, respectively. $\text{LiGaCr}_4\text{O}_8$ with $B_f \sim 0.6$ shows magnetic susceptibility similar to that of conventional Cr spinel oxides such as ZnCr_2O_4 . In contrast, $\text{LiInCr}_4\text{O}_8$ with a small $B_f \sim 0.1$ exhibits a spin-gap behavior in its magnetic susceptibility, suggesting a proximity to an exotic singlet ground state. Magnetic long-range order occurs at 13.8 and 15.9 K for $\text{LiGaCr}_4\text{O}_8$ and $\text{LiInCr}_4\text{O}_8$, respectively, in both cases likely owing to the coupling to structural distortions.

PACS numbers: Valid PACS appear here

Transition metal oxides AB_2O_4 crystallizing in the spinel structure provide us with a rich playground for studying the physics of geometrical frustration. Transition metal *B* atoms, which are octahedrally coordinated by oxide ions, form a three-dimensional network of tetrahedra, i.e., the pyrochlore lattice. Various interesting phenomena have been observed arising from geometrical frustration concerning the spin and charge degrees of freedom on this lattice. Typical examples are the Verwey transition in Fe_3O_4 [1, 2], a heavy-Fermion state in LiV_2O_4 [3], and a heptamer formation in AlV_2O_4 [4].

ACr_2O_4 with a nonmagnetic A^{2+} ion, such as Zn^{2+} , Mg^{2+} , Cd^{2+} , or Hg^{2+} at the tetrahedral site, and Cr^{3+} ions at the octahedral site is of particular interest as a frustrated spin system [5]. It is a Mott insulator with three $3d$ electrons localized at Cr^{3+} , yielding localized $S = 3/2$ Heisenberg spin. Various magnitudes of antiferromagnetic interactions occur between nearest-neighbor spins, as evidenced by a range of negative Weiss temperatures of -390 , -370 , -70 , and -32 K for $A = \text{Zn}$, Mg , Cd , and Hg , respectively [6, 7]. ACr_2O_4 undergoes antiferromagnetic long-range order at 12, 12.4, 7.8, and 5.8 K, respectively [6–8], which is accompanied by a lattice distortion which lowers the crystal symmetry [8–10]. Plausibly, there is an inherent structural instability in the spinel structure that can couple with the spin degree of freedom so as to lift the magnetic frustration.

In this Letter, we study two spinel oxides, $\text{LiGaCr}_4\text{O}_8$ and $\text{LiInCr}_4\text{O}_8$, which both contain two metal ions at the *A* site. Joubert and Durif prepared them in 1966 [11] and found that they crystallize in a modified spinel structure with space group $F\bar{4}3m$, a subgroup of $Fd\bar{3}m$ for the

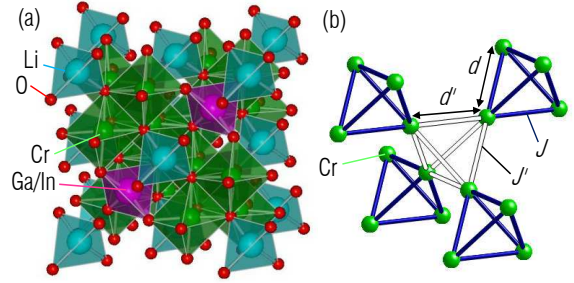


FIG. 1: (color online) (a) Crystal structure of $\text{LiGaCr}_4\text{O}_8$ and $\text{LiInCr}_4\text{O}_8$. Coordination polyhedra made of oxide ions are depicted. (b) Breathing pyrochlore lattice made of Cr^{3+} ions embedded in the two compounds. Cr-Cr bonds on the small (filled sticks) and large tetrahedra (open sticks) have bond lengths d and d' and antiferromagnetic interactions J and J' , respectively.

conventional spinel oxides; an inversion center at the octahedral site present in $Fd\bar{3}m$ is missing in $F\bar{4}3m$. A structural model was proposed in which Li and Ga/In atoms alternately occupy the tetrahedral sites, resulting in the zinc-blende type arrangement, although structural refinements were not performed [11]. This type of *A*-site order is likely, because it minimizes electrostatic energy arising from the large difference in the valence states between Li^+ and $\text{Ga}^{3+}/\text{In}^{3+}$.

We are interested in the Cr pyrochlore lattices of these compounds, because the local chemical pressure caused by the difference in ionic radii of Li^+ and $\text{Ga}^{3+}/\text{In}^{3+}$ should result in the Cr_4 tetrahedra expanding and contracting alternately, whilst keeping their shapes regular,

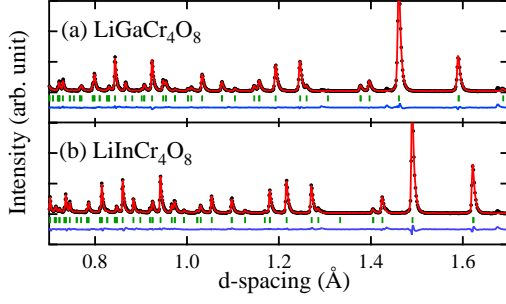


FIG. 2: (color online) Powder neutron diffraction patterns for $\text{LiGaCr}_4\text{O}_8$ (a) and $\text{LiInCr}_4\text{O}_8$ (b) measured on bank 6 ($2\theta = 154^\circ$) of the GEM diffractometer at room temperature. Filled circles are experimental data, and vertical bars indicate the positions of Bragg reflections. The curve on the data shows a calculated pattern, and the bottom curve shows a difference plot between the experimental and calculated intensities.

as shown in Fig. 1(b). We call this type of lattice the “breathing” pyrochlore lattice. The resulting modulation in bond lengths produces two kinds of nearest-neighbor magnetic interactions, J and J' , without relieving frustration. The spin Hamiltonian of the breathing pyrochlore lattice can thus be written as $H = J\sum_{ij}\mathbf{S}_i\cdot\mathbf{S}_j + J'\sum_{ij}\mathbf{S}_i\cdot\mathbf{S}_j$, where the summations over ij in the first and second terms run over the Cr-Cr bonds of small and large tetrahedra, respectively; a uniform pyrochlore antiferromagnet is yielded when $J = J'$, and isolated tetramers are realized for $J' = 0$.

A theoretically predicted ground state for the uniform pyrochlore antiferromagnet is a spin liquid with a finite spin gap [12–14]. This state has not yet been evidenced experimentally because actual compounds always suffer from various perturbations such as lattice deformation or defects. In the weak coupling limit, $J' = 0$, the ground state is also a gapped state, but with a considerably larger gap due to singlet formation on isolated tetrahedra. It would therefore be intriguing to examine how the two states are connected as a function of $B_f = J'/J$ in the breathing pyrochlore lattice. $\text{LiGaCr}_4\text{O}_8$ and $\text{LiInCr}_4\text{O}_8$ are apparently the right compounds to study this issue. The study on the breathing pyrochlore lattice would enable us to get a novel insight on the ground state of the uniform pyrochlore lattice as well as to explore a new phenomenon caused by the breathing.

Polycrystalline samples of $\text{LiGaCr}_4\text{O}_8$ and $\text{LiInCr}_4\text{O}_8$ were prepared by the solid state reaction method. Li_2CO_3 , Cr_2O_3 , and $\text{Ga}_2\text{O}_3/\text{In}_2\text{O}_3$ powders were mixed in 1:4:1 molar ratio, then the mixture was sintered at 1000°C for one day and at 1100°C for another day. Energy dispersive powder neutron diffraction experiments were carried out at room temperature on the General Materials (GEM) diffractometer at the ISIS pulsed neutron source. Rietveld analysis for the structural refine-

TABLE I: Crystallographic parameters for $\text{LiGaCr}_4\text{O}_8$ and $\text{LiInCr}_4\text{O}_8$ (both $F\bar{4}3m$) determined by means of powder neutron diffraction. The lattice constant is $a = 8.2551(7)$ and $8.4205(5)$ Å, respectively. The range of R factors obtained across all banks of data are given, and are found to be consistent with a Le Bail fit of only the main phase. B is the thermal displacement parameter. The following constraints are assumed: $B(\text{Ga1}) = B(\text{Ga2})$, $B(\text{In1}) = B(\text{In2})$, and $B(\text{Li1}) = B(\text{Li2})$.

		x	y	z	Occ.	B (Å ²)
$\text{LiGaCr}_4\text{O}_8$ ($R_p = 3.72\text{--}4.77$, $R_{wp} = 4.79\text{--}6.49$)						
Li1	4a	0	0	0	0.994(7)	1.96(24)
Ga1	4a	0	0	0	0.006(7)	0.53(4)
Li2	4d	3/4	3/4	3/4	0.006(7)	1.96(24)
Ga2	4d	3/4	3/4	3/4	0.994(7)	0.53(4)
Cr	16e	0.3728(3)	x	x	1	0.33(3)
O1	16e	0.13649(14)	x	x	1	0.44(3)
O2	16e	0.61889(13)	x	x	1	0.37(3)
$\text{LiInCr}_4\text{O}_8$ ($R_p = 4.12\text{--}5.84$, $R_{wp} = 5.92\text{--}7.11$)						
Li1	4a	0	0	0	0.992(11)	1.09(28)
In1	4a	0	0	0	0.008(11)	0.35(11)
Li2	4d	3/4	3/4	3/4	0.008(11)	1.09(28)
In2	4d	3/4	3/4	3/4	0.992(11)	0.35(11)
Cr	16e	0.3719(3)	x	x	1	0.14(3)
O1	16e	0.1377(2)	x	x	1	0.38(4)
O2	16e	0.61069(14)	x	x	1	0.18(4)

ment was performed using the Fullprof program on 4 out of the 6 constant angle banks of experimental data using common structural parameters. Magnetic susceptibility and heat capacity measurements were performed in an MPMS and PPMS (both Quantum Design), respectively.

Powder neutron diffraction patterns taken at room temperature for polycrystalline samples of $\text{LiGaCr}_4\text{O}_8$ and $\text{LiInCr}_4\text{O}_8$ are shown in Fig. 2. In addition to reflections expected for $F\bar{4}3m$, forbidden reflections that are allowed for $F\bar{4}3m$, such as 002, are observed. Rietveld refinements using data from 4 banks were attempted starting from either case of full occupation of Li at the 4a site and Ga/In at the 4d site, as in the case of $\text{LiFe}_2\text{Rh}_3\text{O}_8$ [15], or vice versa. Irrespective of the initial conditions, the refinements converged in a model in which the 4a and 4d sites are fully occupied by Li and Ga/In, respectively, within error bars. This is consistent with the model by Joubert and Durif [11]. Details of the refinement are given in Table I. The lattice parameters obtained are $8.2551(7)$ and $8.4205(5)$ Å, respectively, which are similar to $8.243(3)$ and $8.411(3)$ Å reported previously [11]. Thus, we have confirmed that the $F\bar{4}3m$ model with perfect A-site order is appropriate for the two compounds and successfully obtained reliable atomic coordinates.

The zinc blende type order of small Li^+ and large $\text{Ga}^{3+}/\text{In}^{3+}$ ions on the 4a and 4d sites gives rise to a local chemical pressure on the Cr pyrochlore lattice, resulting in an alternation of the size of the Cr_4 tetrahe-

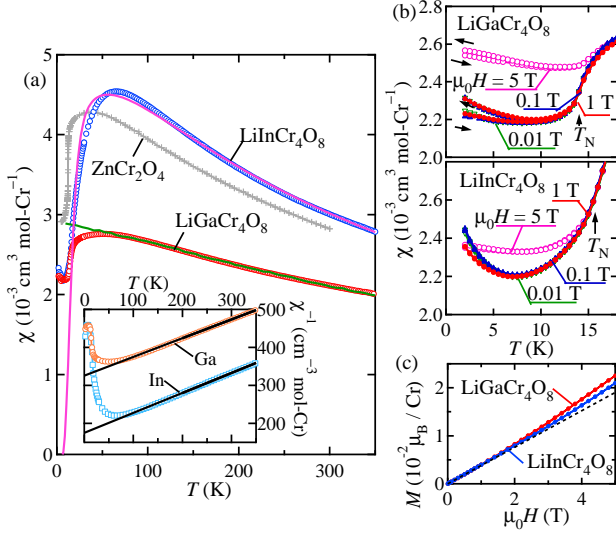


FIG. 3: (color online) (a) Temperature dependence of magnetic susceptibility χ measured in a magnetic field of 1 T for polycrystalline samples of $\text{LiGaCr}_4\text{O}_8$ and $\text{LiInCr}_4\text{O}_8$. The data for a polycrystalline sample of ZnCr_2O_4 are also shown for comparison [6]. Solid lines are calculated curves produced by classical Monte Carlo simulations with $J' = 0.5J$ ($J = 53.3$ K) for the Ga data and by the exact result for an isolated tetrahedron ($J = 56.8$ K) for the In data. The inset shows inverse susceptibilities with Curie-Weiss fits. (b) Temperature dependences of field-cooled and zero-field-cooled χ 's measured at various magnetic fields for $\text{LiGaCr}_4\text{O}_8$ (upper) and $\text{LiInCr}_4\text{O}_8$ (lower). (c) M - H curves for $\text{LiGaCr}_4\text{O}_8$ and $\text{LiInCr}_4\text{O}_8$ measured at 5 K. The broken line shows an initial straight line.

dra. The Cr-Cr distances of the small and large tetrahedra, denoted as d and d' , are found to be 2.867(4) and 2.970(4) Å for $\text{LiGaCr}_4\text{O}_8$, and 2.903(4) and 3.052(4) Å for $\text{LiInCr}_4\text{O}_8$, respectively. The differences between d and d' are 3.5% and 4.9%, respectively, meaning a stronger alternation or breathing in $\text{LiInCr}_4\text{O}_8$ than in $\text{LiGaCr}_4\text{O}_8$.

Figure 3(a) shows the temperature dependence of magnetic susceptibility χ for $\text{LiGaCr}_4\text{O}_8$ and $\text{LiInCr}_4\text{O}_8$. The inverse of χ , shown in the inset, exhibits a linear temperature dependence above ~ 100 K, following the Curie-Weiss law $\chi = C/(T - \theta_W)$, where C and θ_W are the Curie constant and the Weiss temperature; a fit to the data between 200 and 350 K yields $C = 2.025(3) \text{ cm}^3 \text{ K mol-Cr}^{-1}$ and $\theta_W = -658.8(4) \text{ K}$ for $\text{LiGaCr}_4\text{O}_8$, and $C = 1.899(4) \text{ cm}^3 \text{ K mol-Cr}^{-1}$ and $\theta_W = -331.9(4) \text{ K}$ for $\text{LiInCr}_4\text{O}_8$. The values of C correspond to effective moments of $\mu_{\text{eff}} = 4.024 \mu_B$ and $3.897 \mu_B$ per Cr atom, or Lande g -factors of $g = 2.078$ and 2.012 for $S = 3/2$, respectively. The large and negative θ_W indicates that average magnetic interactions are strongly antiferromagnetic.

The χ versus T curve of $\text{LiGaCr}_4\text{O}_8$ resembles that of

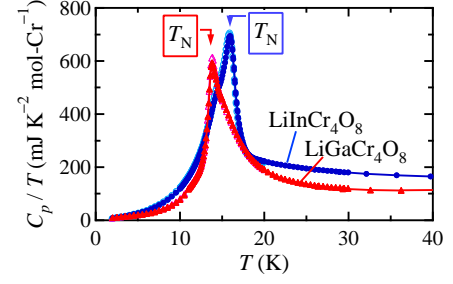


FIG. 4: (color online) Temperature dependence of heat capacity divided by temperature C_p/T for polycrystalline samples of $\text{LiGaCr}_4\text{O}_8$ and $\text{LiInCr}_4\text{O}_8$. Filled and open symbols represent data measured at magnetic fields of 0 and 9 T for each sample, respectively.

ZnCr_2O_4 , as indicated in Fig. 3(a). It shows a broad peak at ~ 45 K, which represents a development of antiferromagnetic short-range order. In the case of ZnCr_2O_4 , the corresponding broad peak appears at ~ 30 K, reflecting stronger magnetic interactions in $\text{LiGaCr}_4\text{O}_8$. On further cooling, χ decreases steeply at ~ 14 K, where long-range order sets in, as also evidenced by a sharp peak in heat capacity at $T_N = 13.8$ K (Fig. 4), close to that of ZnCr_2O_4 . Therefore, the breathing of the pyrochlore lattice in $\text{LiGaCr}_4\text{O}_8$ has little influence on the magnetic properties.

In contrast, the χ of $\text{LiInCr}_4\text{O}_8$ shows a temperature dependence which is obviously distinguishable from that of the Ga analogue: it rapidly decreases with decreasing temperature below 65 K, which is reminiscent of the opening of a spin gap. The gap size is roughly estimated to be $\Delta = 56.8(2) \text{ K}$ by a fit to the exact result for an isolated tetrahedron of $S = 3/2$, where the diamagnetic contribution of core electrons of $-4.0 \times 10^{-5} \text{ cm}^3 \text{ mol-Cr}^{-1}$ is included [16], as shown in Fig. 3(a). At yet lower temperature, a sharp peak in C_p/T (Fig. 4) indicates long-range order at $T_N = 15.9 \text{ K}$. Based on this, we believe the ground state of $\text{LiInCr}_4\text{O}_8$ to be in proximity to a spin-gapped state, despite the long-range order at low temperature. As shown in Fig. 3(b), the χ of each compound is nearly insensitive to magnetic fields below 1 T, beyond which it suddenly increases at 5 T below T_N . This is clearly observed in the M - H curves shown in Fig. 3(c), where an upturn from the initial straight line appears at approximately 2 T in each compound. This may be due to a spin flop transition in the ordered state.

We now consider magnetic interactions in the Cr spinel oxides. Generally, it is well established that the shorter the Cr-Cr distance, the stronger the antiferromagnetic interaction, as shown in Fig. 5, because exchange interactions are dominantly mediated by direct overlap between Cr t_{2g} orbitals along the Cr-Cr bond [17, 18]. For example, the J of ZnCr_2O_4 is 33-45 K [19-21], almost ten times larger than 4 K for HgCr_2O_4 [7, 22], which comes from

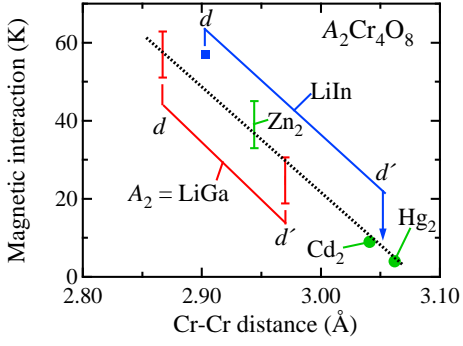


FIG. 5: (color online) Nearest-neighbor magnetic interaction versus the Cr-Cr distance for various Cr spinel oxides. The J value of ZnCr_2O_4 are estimated by fitting χ , C_p , and EPR intensity [19–21]. The J 's of CdCr_2O_4 and HgCr_2O_4 are estimated by Curie-Weiss fits to χ [6, 7, 22]. The dotted line is a guide for the eyes. Plotted for $\text{LiGaCr}_4\text{O}_8$ or $\text{LiInCr}_4\text{O}_8$ is a pair of points corresponding to the two Cr-Cr distances in the small and large tetrahedra.

a 4% difference in the Cr-Cr distance between ZnCr_2O_4 (2.944 Å) and HgCr_2O_4 (3.062 Å). Interestingly, there is an approximate linear relationship between J and the bond length for ACr_2O_4 , as indicated by the dotted line in Fig. 5.

A remarkable feature of the present Ga and In compounds is the extremely short Cr-Cr distance within the small Cr_4 tetrahedra compared with that of ACr_2O_4 : $d = 2.867$ Å (Ga) and 2.903 Å (In) are much shorter than 2.944 Å in ZnCr_2O_4 [23], suggesting that J in the Ga and In compounds are larger than $J = 33\text{--}45$ K in ZnCr_2O_4 . On the other hand, the distance $d' = 2.970$ Å within the large tetrahedra of $\text{LiGaCr}_4\text{O}_8$ is comparable to the Cr-Cr distance of ZnCr_2O_4 , while the $d' = 3.052$ Å for $\text{LiInCr}_4\text{O}_8$ lies between 3.041 Å in CdCr_2O_4 and 3.062 Å in HgCr_2O_4 . Assuming that the linear relationship observed in ACr_2O_4 holds in $\text{LiGaCr}_4\text{O}_8$ and $\text{LiInCr}_4\text{O}_8$, we arrive at estimates of $J \sim 60$ and 50 K and $J' \sim 30$ and 6 K, which give a breathing factor $B_f = J'/J \sim 0.5$ and 0.12 , respectively.

To more accurately estimate J and J' , we carried out fitting of the χ data shown in Fig. 3(a). Classical Monte Carlo simulations were performed using the spinmc program of the ALPS package (1024 sites, periodic boundary conditions). Although it was difficult to determine the two values uniquely, we could obtain J for various B_f 's, e.g. $J = 62.9(5)$, $53.3(1)$, and $51.0(3)$ K for $B_f = 0.3$, 0.5 , and 0.6 , respectively; a typical fitting curve for $B_f = 0.5$ is shown in Fig. 3(a). Taking into account of $J \sim 50$ K from the universal line in Fig. 5, we decide $B_f = 0.6$ for $\text{LiGaCr}_4\text{O}_8$.

In contrast to $\text{LiGaCr}_4\text{O}_8$, the fit to the Monte Carlo results was poor for $\text{LiInCr}_4\text{O}_8$. Thus, we adopt $J = 56.8(2)$ K from the fitting to the exact result mentioned

before, which lies close to the universal line in Fig. 5. We also tried to fit the data by taking account of J' in the mean-field approximation. However, the improvement of fitting was limited, and it resulted in an unreasonably large ferromagnetic J' . Thus, we assume $J' \sim 6$ K from the universal relation in Fig. 5, which gives $B_f \sim 0.1$ for $\text{LiInCr}_4\text{O}_8$. The breathing factor can be an important parameter to tune the ground state of pyrochlore lattice antiferromagnets.

Finally, we describe the characteristics of the ordering transitions in the two compounds. Their C_p/T curves, shown in Fig. 4, exhibit sharp peaks at 13.8 and 15.9 K, respectively, clear evidence for magnetic transitions. Interestingly, the peak shape for $\text{LiGaCr}_4\text{O}_8$ is apparently different from that of a conventional second-order magnetic transition: the C_p/T shows a broad shoulder at ~ 16 K above T_N and gradually decreases with increasing temperature, indicating that a large spin entropy is retained above T_N due to the development of antiferromagnetic short-range order. In $\text{LiInCr}_4\text{O}_8$, there is also a large entropy release above T_N , associated with a spin-gap formation. These magnetic transitions are quite robust against magnetic fields: the two C_p/T curves measured at 0 and 9 T nearly overlap to each other in each compound.

The origin of long-range order in the present two compounds is not perfectly confirmed. In the absence of structural distortions, geometrical frustration should remain and favor a spin-liquid ground state. In ACr_2O_4 , a structural transition always takes place simultaneously with the magnetic transition. The similar T_N 's of $5\text{--}15$ K, in spite of the broad variation of J , suggest a common structural instability that is coupled with spins through strong spin-lattice interactions. This is also likely the case for the present compounds. We plan to investigate the crystal and magnetic structures across T_N by means of NMR, X-ray, and neutron diffraction experiments. Moreover, inelastic neutron scattering experiments will aid in establishing the presence (or absence) of a gap in either material, as well as allowing for quantitative determination of J and J' . Although the compounds assume long-range ordered ground states, fingerprints of neighboring spin liquid states or the effect of frustration may be observable as in Ref. 24 and 25.

In summary, two spinel oxides $\text{LiGaCr}_4\text{O}_8$ and $\text{LiInCr}_4\text{O}_8$ with the tetrahedral sites alternately occupied by Li^+ and $\text{Ga}^{3+}/\text{In}^{3+}$ ions are found to be unique frustrated antiferromagnets with breathing pyrochlore lattices. $\text{LiGaCr}_4\text{O}_8$, with a lesser degree of breathing, shows similar magnetic properties to the conventional Cr spinel oxides with a uniform pyrochlore lattice, while $\text{LiInCr}_4\text{O}_8$ shows a spin-gap behavior caused by a large alternation of magnetic interactions in the more breathing pyrochlore lattice. The breathing of the pyrochlore lattice appears to be an important parameter to explore interesting phenomena in frustrated magnets.

We thank H. Tsunetsugu, M. Isobe, H. Ueda, and T.

Nakazono for helpful discussion.

-
- [1] E. J. W. Verwey, *Nature (London)* **144**, 327 (1939).
 - [2] M. S. Senn, J. P. Wright, and J. P. Attfield, *Nature (London)* **481**, 173 (2012).
 - [3] S. Kondo, D. C. Johnston, C. A. Swenson, F. Borsa, A. V. Mahajan, L. L. Miller, T. Gu, A. I. Goldman, M. B. Maple, D. A. Gajewski, E. J. Freeman, N. R. Dilley, R. P. Dickey, J. Merrin, K. Kojima, G. M. Luke, Y. J. Uemura, O. Chmaissem, and J. D. Jorgensen, *Phys. Rev. Lett.* **78**, 3729 (1997).
 - [4] Y. Horibe, M. Shingu, K. Kurushima, H. Ishibashi, N. Ikeda, K. Kato, Y. Motome, N. Furukawa, S. Mori and T. Katsufuji: *Phys. Rev. Lett.* **96**, 086406 (2006).
 - [5] S.-H. Lee, H. Takagi, D. Louca, M. Matsuda, S. Ji, H. Ueda, Y. Ueda, T. Katsufuji, J.-H. Chung, S. Park, S.-W. Cheong, and C. Broholm: *J. Phys. Soc. Jpn.* **79**, 011004 (2010).
 - [6] H. Ueda, H. A. Katori, H. Mitamura, T. Goto, and H. Takagi: *Phys. Rev. Lett.* **94**, 047202 (2005).
 - [7] H. Ueda, H. Mitamura, T. Goto, and Y. Ueda: *Phys. Rev. B* **73**, 094415 (2006).
 - [8] L. Ortega-San-Martín, A. J. Williams, C. D. Gordon, S. Klemme, and J. P. Attfield: *J. Phys. Condens. Matter* **20**, 104238 (2008).
 - [9] S.-H. Lee, C. Broholm, T. H. Kim, W. Ratcliff II, and S.-W. Cheong: *Phys. Rev. Lett.* **84**, 3718 (2000).
 - [10] J.-H. Chung, M. Matsuda, S.-H. Lee, K. Kakurai, H. Ueda, T.J.Sato, H. Takagi, K.-P. Hong, and S. Park: *Phys. Rev. Lett.* **95**, 247204 (2005).
 - [11] J.-C. Joubert and A. Durif: *Bull. Soc. franç. Minér. Crist.* **89**, 26 (1966).
 - [12] H. Tsunetsugu: *J. Phys. Soc. Jpn.* **70**, 640 (2001).
 - [13] A. B. Harris, A. J. Berlinsky, and C. Bruder: *Appl. Phys. Lett.* **69**, 5200 (1991).
 - [14] B. Canals and C. Lacroix: *Phys. Rev. Lett.* **80**, 2933 (1998).
 - [15] K. U. Kang and C. S. Kim: *Hyperfine Interactions* **168**, 1181 (2006).
 - [16] R. R. Gupta: *Landolt-Börnstein* (Springer, Berlin, 1986) New Series, Group II, Vol. 16, p. 402.
 - [17] T. Rudolf, Ch. Kant, F. Mayr, J. Hemberger, V. Tsurkan, and A. Loidl: *New J. Phys.* **9**, 76 (2007).
 - [18] A. N. Yaresko: *Phys. Rev. B* **77**, 115106 (2008).
 - [19] H. Martinho, N. O. Moreno, J. A. Sanjurjo, C. Rettori, A. J. García-Adeva, D. L. Huber, S. B. Oseroff, W. Ratcliff II, S.-W. Cheong, P. G. Pagliuso, J. L. Sarrao, and G. B. Martins: *Phys. Rev. B* **64**, 024408 (2001).
 - [20] Ch. Kant, J. Deisenhofer, T. Rudolf, F. Mayr, F. Schrettle, A. Loidl, V. Gvezdilov, D. Wulferding, P. Lemmens, and V. Tsurkan: *Phys. Rev. B* **80**, 214417 (2009).
 - [21] A. J. García-Adeva and D. L. Huber: *Phys. B* **320**, 18 (2002).
 - [22] H. Ueda, J. Yamaura, H. Mitamura, T. Goto, H. A. Katori, H. Takagi, and Y. Ueda: *J. Mag. Mag. Mater.* **310**, 1275 (2007).
 - [23] H. Sawada: *Mat. Res. Bull.* **32**, 873 (1997).
 - [24] S.-H. Lee, C. Broholm, W. Ratcliff, G. Gasparovic, Q. Huang, T. H. Kim, and S.-W. Cheong: *Nature (London)* **418**, 856 (2002).
 - [25] K. Tomiyasu, H. Suzuki, M. Toki, S. Itoh, M. Matsuura, N. Aso, and K. Yamada: *Phys. Rev. Lett.* **101**, 177401 (2008).

* email address: yokamoto@issp.u-tokyo.ac.jp

† present address: Institut Laue-Langevin, 6 rue Jules Horowitz, Boîte Postale 156, 38042 Grenoble Cedex 9, France.